

Centrifuge Shaking Table Tests and FEM Analyses of RC Pile Foundation and Underground Structure



Kenji Yonezawa

Obayashi Corporation, Tokyo, Japan.

Takuya Anabuki

Obayashi Corporation, Tokyo, Japan.

Shunichi Higuchi

Obayashi Corporation, Tokyo, Japan.

Joji Ejiri

Obayashi Corporation, Tokyo, Japan.

SUMMARY:

Three cases of centrifuge shaking table tests with 1/25 scaled models of a RC pile foundation and a RC box culvert installed in the grounds were conducted to obtain foundational data for verifying applicability of nonlinear FEM analysis method in consideration of soil-structure interaction. In the two cases, the influence of the ground condition on the nonlinear responses of structure was investigated by using the pile foundation models. In the third case, the influence by existence of a contiguous structure was evaluated by using the RC box culvert model installed close to the pile foundation. Furthermore, nonlinear finite element analyses were conducted for the two cases of the tests. By comparing the test results and analysis results, it was confirmed that nonlinear responses of both the ground and the structures were reasonably reproduced by the analysis.

Keywords: Centrifuge shaking table Test, Underground Structure, Pile Foundation, FEM Analysis

1. INTRODUCTION

Recently, it is desirable that nonlinear responses of structures are clarified by soil-structure interaction analysis, especially for evaluating the seismic performances of underground structure or foundation because a more severe seismic action has been assumed on the seismic design after the experience of the 1995 Hyogoken Nanbu Earthquake. Finite element method has been employed actively to evaluate the dynamic response of the underground structure and the foundation. But few reports verified applicability and accuracy of the FEM analysis for evaluating the inelastic structure behaviours in consideration of soil-structure interaction by comparison of test results and analysis results.

In this research, three cases of centrifuge shaking table tests using 1/25 scaled models of a reinforced concrete pile foundation and a RC box culvert installed in the ground were carried out to obtain foundational data for verification of nonlinear FEM analysis method in consideration of soil-structure interaction. In the two cases, influence of the ground condition on the nonlinear responses of structure was investigated by using the pile foundation models. In the other case, influence by existence of a contiguous structure was evaluated by using the RC box culvert model which installed close to the pile foundation in the dry ground. Then, finite element analyses for the two tests were conducted to confirm an applicability of the analytical method.

This paper describes outline of the tests, the analysis methods and their results, then discusses the nonlinear seismic responses of the structure under the ground and the applicability of the analysis.

2. CENTRIFUGE VIBRATION TEST

The aim of the centrifuge shaking table tests was to obtain the fundamental data for verification of the analysis methods. Three cases were conducted under the 25G centrifugal gravity in this study. The

1/25 scaled models of the RC pile foundations, the RC box culvert and the ground were used in the tests. The RC pile foundations installed in the dry ground and in the liquefied ground were used in the Case1 and Case2 respectively. In the Case3, The RC box culvert was installed close to the RC pile foundation in the dry ground. In this case, in order to investigate influence of the contiguous structure, the model ground was divided into two sections by steel plate as shown in **Figure 1**. One of the sections installed the pile foundation and the box culvert, the other section installed only box culvert. **Figure 1** shows the profiles of specimen and instrumentation plans of the three test cases.

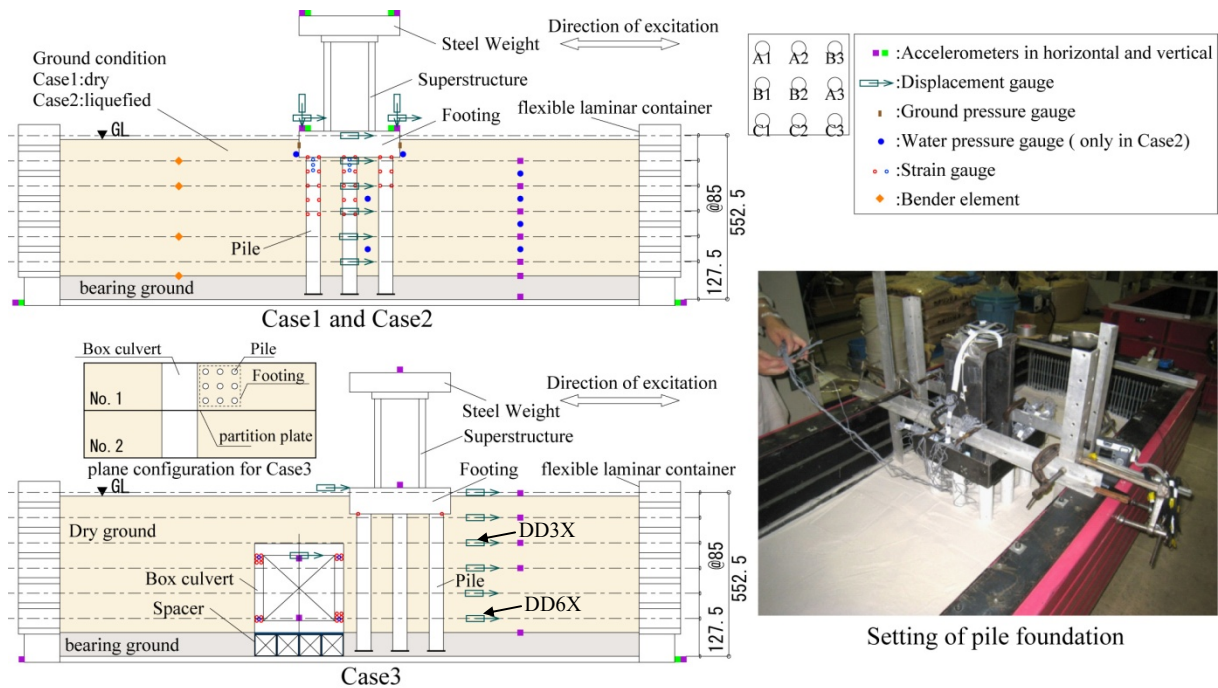


Figure 1. Profiles of specimen and instrumentation plans

2.1. Model preparations

2.1.1. RC pile foundation model

The RC pile foundation used in the tests was made as 1/25 scaled model of a pile foundation under a bridge pier shown in **Figure 2**. The RC pile foundation consisted of a footing with a square section (340mm x 340mm) and nine piles with 48mm in diameter. Configuration of the RC pile foundation model is shown in **Figure 2**. It was composed of the fine reinforcing bars and the concrete with 1/25-scaled-down fine and coarse aggregates employed (hereafter, micro-concrete). Longitudinal reinforcing bars in a pile were eight deformed bars with 1.9mm in diameter. Transverse reinforcement in the piles was circular hoops of deformed bars with 0.7mm in diameter with spacing of 6mm in the upper part and 12mm in the general part. The reinforcing arrangement is also shown in **Figure 2**. Material properties of the reinforcing bars and micro-concrete are shown in **Table 1** and **Table 2**, respectively.

The footing consisted of high strength mortar and steel plate forms of 3.2mm thickness. The head of the piles was put through the holes made in the bottom plate, and then the mortar concrete was poured into the footing. Thus, the connection between the footing and the pile head was assumed to be rigid. A superstructure consisted of steel plate portal frame and steel weight of about 587N (About 1000ton in prototype) located on the superstructure. Bottom of the superstructure was rigidly welded to the bottom plate of the footing.

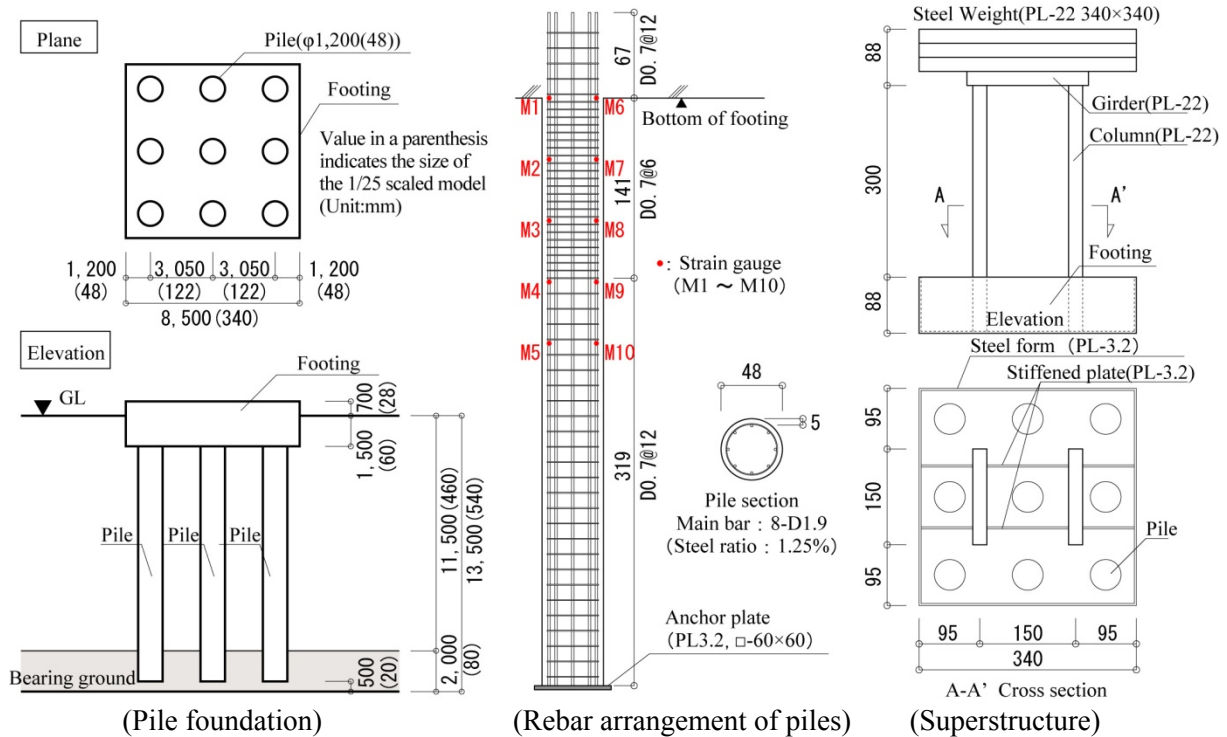


Figure 2. Configuration of pile foundation model

2.1.2. RC underground structure model

The underground structure used in the tests was made as 1/25 scaled model of a box culvert as shown in **Figure 1** and **Figure 3**. The dimension and reinforcing arrangement of the model are also shown in **Figure 3**. The configuration of inner space was 220mm high and 220mm width (5.5m by 5.5m in prototype scale) and the thickness of sidewalls is 30mm (0.75m in prototype scale). It was composed of the fine reinforcing bars and the micro-concrete, as same as the pile foundation. Longitudinal reinforcing bars in upper and lower slab were deformed bars with 1.9mm in diameter. Main reinforcing bars in the wall, transverse reinforcements and distributing bars were the deformed bars with 1.0mm in diameter. The material properties of micro-concrete and reinforcing bars are shown in **Table 1** and **Table 2**, respectively. The box culvert was connected to the bottom of the container rigidly by using steel spacer of 80mm height because of assumption that the box culvert was fixed to bed rock.

Prior to the centrifuge shaking table tests, a reversed cyclic loading test of the box culvert was also conducted to obtain its deformation characteristic. **Figure 4** shows a load – drift angle relationship obtained from the test.

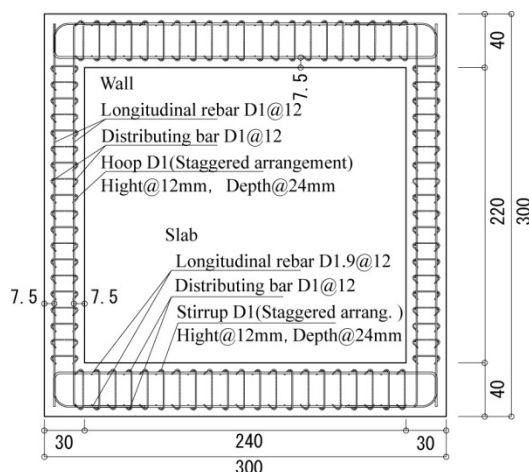


Figure 3. Configuration of box culvert

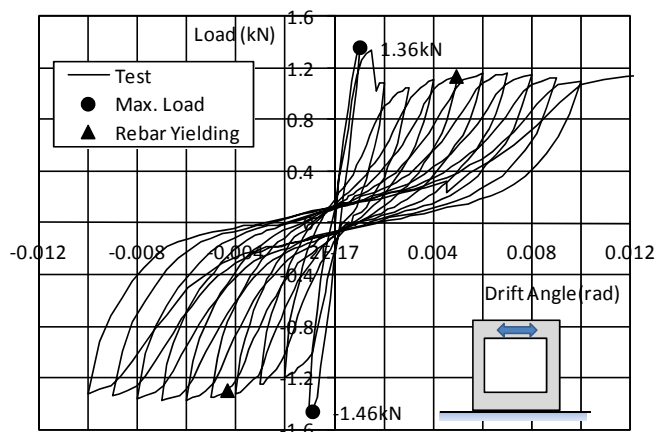


Figure 4. Load – drift angle relationship of static test

Table 1. Material properties of rebars

	Young's Modulus	Yield Strength	Tensile Strength
D0.7	2.16×10^5	415	417
D1.9 in Pile	1.85×10^5	314	322
D1.0	1.85×10^5	304	325
D1.9 in culvert	2.14×10^5	391	404

Table 2. Material properties of micro concrete

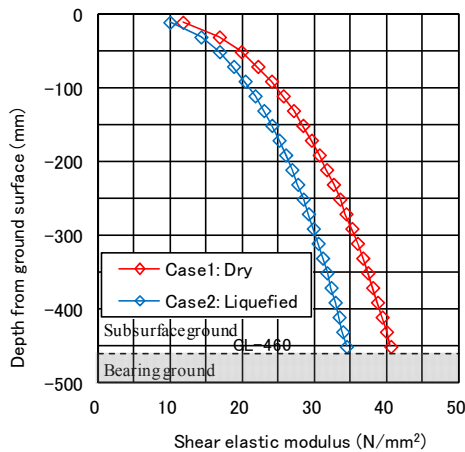
	Young's Modulus	Compressive Strength	Cleavage Strength
Case1	2.92×10^4	35.0	2.93
Case2	2.71×10^4	24.6	1.76
Case3	2.75×10^4	31.4	2.02

Unit : N/mm²

2.1.3. Preparation of the ground

Model grounds, consisted of fine silica sand ($D_{50}=0.1\text{mm}$), were prepared in the flexible container by the air pluviation method, with its dimensions of 1950mm long, 800mm in width and 550mm deep (equivalent to 48.75m long, 20m in with and 13.75m deep respectively in prototype scale). Dry density of 1.45t/m^3 ($Dr=84\%$) was achieved for the dry ground cases (Case1 and Case3), and submerged density of 1.88t/m^3 ($Dr=63\%$) for the saturated ground case (Case2). Methylcellulose solution ($25\text{mPa}\cdot\text{s}$), used as pore fluid to satisfy the similitude of pore water dissipation on the saturated ground, was poured into the ground by the ground surface. Cement mixed soil was used for the base stratum under the sand ground. Because it is assumed as the bearing stratum for the pile foundation, shear wave velocity of the base stratum was set about 300-400 m/s.

Figure 5 shows initial shear modulus distributions of the ground measured by on fricht bender element measurements in Case1 and Case2. Material properties of the base stratum and the subsurface stratum are shown in **Table 3** and **Table 4**, respectively.

**Figure 5.** Shear elastic modulus distribution**Table 3.** Material properties of bearing ground

	Young's Modulus N/mm ²	Compressive Strength N/mm ²	Cleavage Strength N/mm ²
Case1	5.16×10^2	2.58	0.28
Case2	3.17×10^3	1.31	0.13
Case3	3.24×10^3	1.51	

Table 4. Material properties of subsurface ground

Measuring Range	Shear Wave Velocity m/s	Shear Elastic Modulus N/mm ²
GL-72.5~GL-157.5	133	25.6
GL-327.5~GL-460	163	38.7

2.2. Test sequence

At first, the centrifugal gravity of 25G was given to the test specimen. Then, the horizontal motions were given by using ground acceleration time history observed at the Port-island, KOBE in the 1995 Hyogoken Nanbu Earthquake. Six excitations, of which amplitude of the input acceleration increased in stages, were conducted in each three cases of the tests. The lists of maximum response acceleration at the shaking table measured in all the tests are shown in **Table 5**. **Figure 6** shows a time history of response acceleration on the shaking table of No.d6 in the Case3.

2.3. Data measurement

Locations of measuring instrumentations were shown in **Figure 1**. Accelerations on the shaking table, in the ground, top of the footing, and top of the superstructure were measured. Relative displacements of each container laminas and box culvert, absolute displacements on top of the footing, strains of the reinforcing bars, soil pressure on side of the footing were also measured in the tests. On fricht measurement of the ground shear wave velocities was conducted by the bender elements. In addition, pore-water pressures in the ground were measured in the Case2 with liquefied ground.

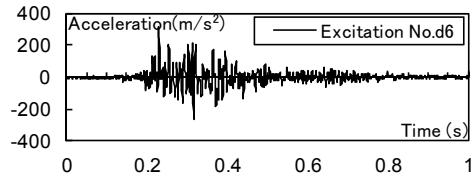


Figure 6. Example of acceleration input (Case3, d6)

Table 5. Maximum acceleration of input (Unit: m/s^2)

	d1	d2	d3	d4	d5	d6
Case1	2.9	2.8	91.7	119.7	185.1	262.6
Case2	5.9	10.7	22.4	64.0	168.0	223.8
Case3	25.8	43.8	88.1	66.9	186.5	315.6

2.4. Test results

2.4.1. Results of Case 1 and Case2

The test results were summarized by comparing the responses from in representative excitations of No.d6 in both cases.

Figure 7 compares time histories of horizontal acceleration measured on the top of the superstructure. In Case 1 with dry ground, long period components were appeared in comparison with Case2 with liquefied ground. It was also seen that the acceleration of Case 1 was larger than that of Case2 between about 0.28 and 0.43 second.

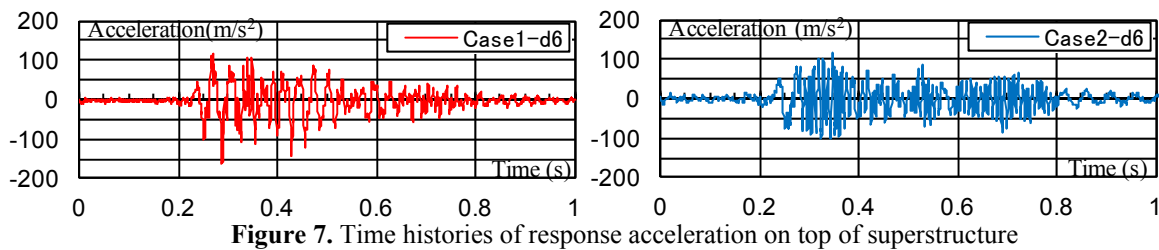


Figure 7. Time histories of response acceleration on top of superstructure

Figure 8 shows time histories of horizontal displacement of the footing. Although the acceleration on top of the superstructure of Case1 was larger than that of Case2, the horizontal displacement of the footing of Case2 was larger than that of Case1. But after excess pore water pressure ratio reached 1.0, the displacement of Case2 became smaller than that of Case1 (see Figure 9). As for this reason, it was inferred that the ground stiffness was reduced due to decreasing the effective stress of the ground by raising excess pore water pressure in the Case2.

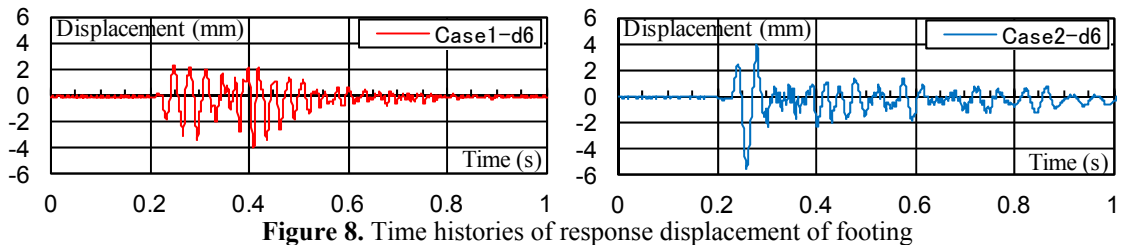


Figure 8. Time histories of response displacement of footing

Figure 9 shows time histories of the excess pore water pressure ratio in the free field and ground between piles. Both of excess pore water pressure ratios were increasing right after excitation start, and reached 1.0 at about 0.3 second. It was also found that the field between the piles belatedly caused liquefaction in comparison with the free field.

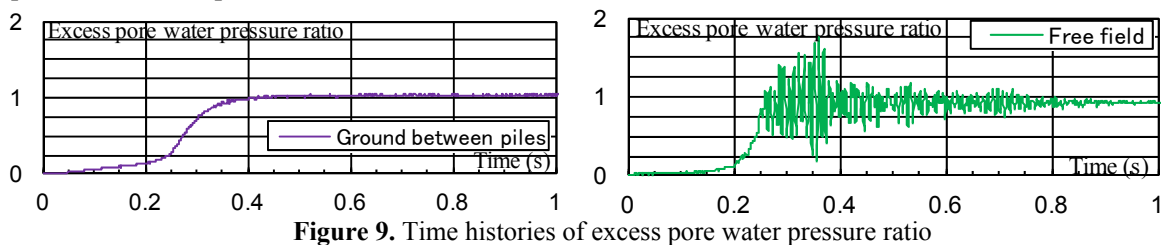


Figure 9. Time histories of excess pore water pressure ratio

2.4.2. Results of Case 3

The test results were summarized as follows by comparing two cases with and without the contiguous structure.

Figure 10 compares time histories of drift angles of the box culvert and shear strain of the ground

obtained from excitation No.d3 and No.d6. Judged from the response of rebars, in the No.d3 excitation, box culvert responded in elastic range. The shear strains of the ground were calculated from the response displacements of the laminar container (used DD3X and DD6X shown in **Figure 1**). On the other hand, in the No.d6 excitation, reinforcing bars of the box culvert yielded as shown in **Figure 11**. By comparing between two cases with and without the pile foundation in the excitations No.d3 when the box culvert remained in elastic range, it was found that both the periods of vibration were different between the time of 0.3s and 0.5s, and the drift angle of the case without the pile foundation was larger than that of the case with the pile foundation. As the results, it was confirmed that behavior of the underground structure was influenced by the existence of the contiguous structure, under the small excitation in which the structure remained in elastic range. On the other hand, as for the responses characteristic in the No.d6 excitation in which both the ground and the structure reached plastic range, the difference between two cases was not remarkable. Therefore, under large excitation levels in which both the ground and the structure reached plastic range, it was found that influence of the contiguous structure was not remarkable. The reason was that the difference of stiffness between the structure and the ground became small with yielding of reinforcing bar and cracking of the concrete.

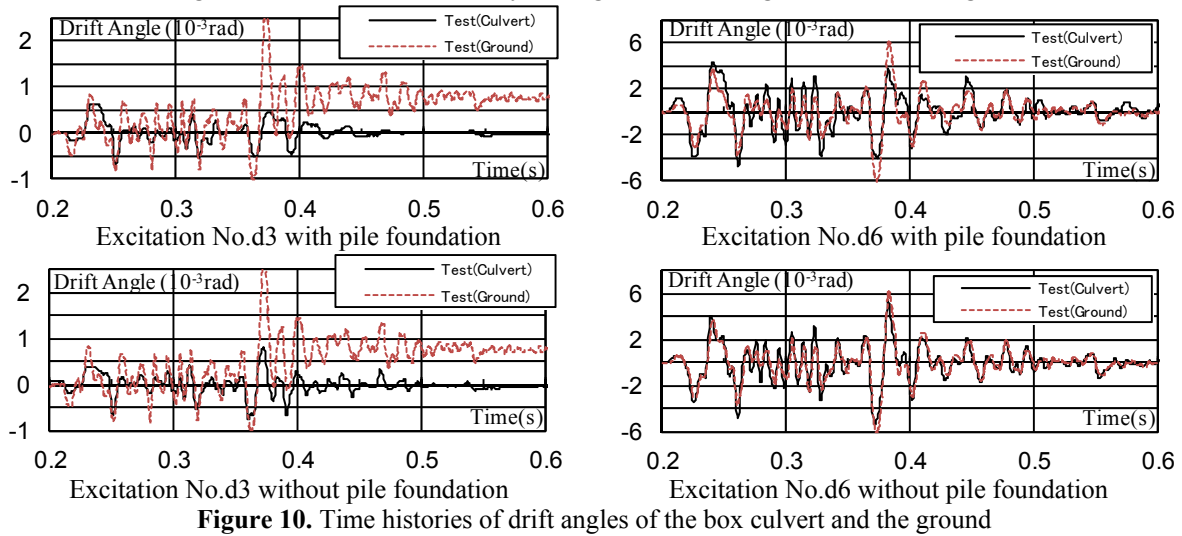


Figure 10. Time histories of drift angles of the box culvert and the ground

Figure 11 compares the time histories of the reinforcing bar strain of the box culvert obtained from the two cases with and without the pile foundation, in the No.d6 excitation. In both cases, the strains of the reinforcement bars reached the yield strain (yielded strain: 0.164%). On the response of the reinforcing bar in the No.6 excitation in which both the ground and the structure reached plastic range, the influence of the existence of the contiguous structure was also found to be not remarkable like the response of the drift angle.

Figure 12 shows the damaged conditions of the box culverts observed from two cases after the test. The crack patterns of two cases were almost the same. It was confirmed that flexural cracks appeared at the both ends of the wall in the both cases.

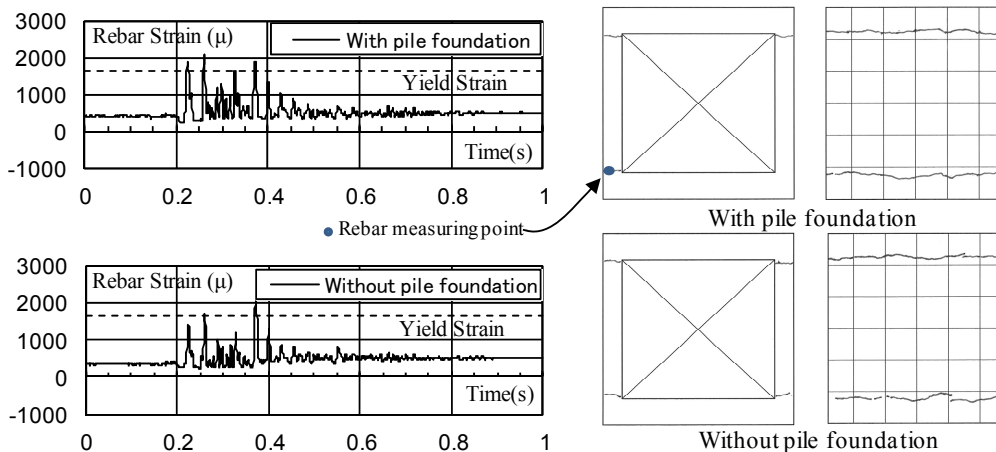


Figure 11. Time histories of rebar strain (No.d6)

Figure 12. Damaged conditions after the test

3. NONLINEAR FINITE ELEMENT ANALYSES FOR THE CENTRIFUGE TESTS

Three dimensional FEM analyses for the Case1 and Case3 with the dry ground were conducted. Outlines and results of the analyses are described below. Computer code used here was “FINAL-GEO” developed by Obayashi Corporation.

3.1. Outline of the 3D FEM analyses

3.1.1. Modelling

Figure 13 shows the analysis models for Case1 and Case3. Concrete and ground were represented by hexahedral elements and longitudinal and transverse reinforcing bars were modelled by truss elements. For taking into account the interaction between the concrete and the ground, joint elements were inserted on the pile surface and bottom of the footing. As for the total number of nodes, the model of Case1 was 167,729, and that of Case3 was 165,610. As for the total number of DOF (Degree of Freedom), the model of Case1 was 482,764, and that of Case3 was 480,086.

3.1.2. Boundary condition and input motions

For taking into account the behaviour of the flexible laminar container, weight and shear stiffness of the container were represented by applying the nodal mass, shear spring, and function of dependent DOF, on the both side surfaces of the models, as shown in **Figure 14**. Vertical nodal displacements on both side surfaces were assumed to be free. Bottom surface of the models was completely fixed. The analyses were continuously conducted for the excitations from No.d4 through No.d6. As for the analysis input motions, the accelerations time histories on the shaking table measured in those excitations were applied in the horizontal direction after the vertical force corresponding centrifugal self weight force of 25G was applied.

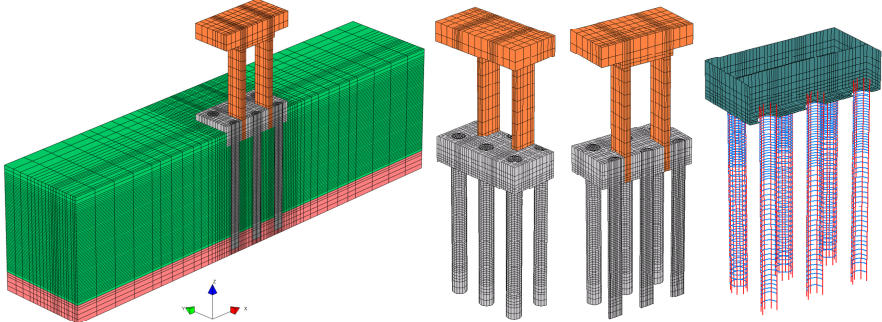


Figure 13(a). Analysis model for Case1

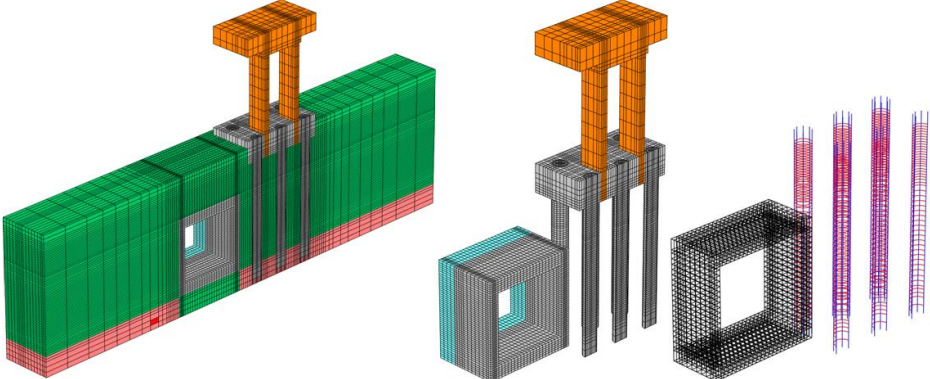


Figure 13(b). Analysis model for Case3

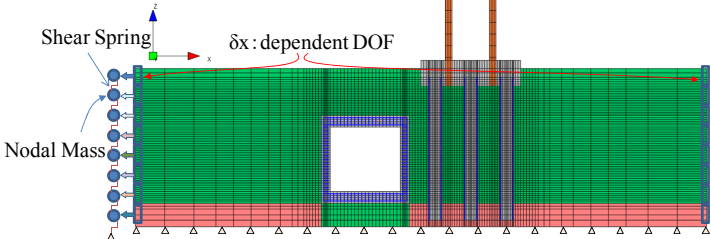


Figure 14. Idealization of flexible laminar container and boundary condition

3.2. Material constitutive model

3.2.1 Concrete

Concrete is idealized using the orthotropic model based on equivalent uniaxial strain concept. The model employs hypo-elastic constitutive relationships (nonlinear elasticity). The axes of orthotropy coincide with the current principal direction before occurrence of cracking. After cracking, Non-orthogonal multi-directional crack model was applied here.

As for compressive characteristics of concrete, Compressive stress - strain relationship was defined by a modified Ahmad model, which can represent increase of the maximum concrete strength under tri-axial stress state. **Figure 15** shows the stress - strain relationship of concrete.

As for tensile characteristics of concrete, tensile stress - strain relationship was assumed to be linear up to cracking, and tension stiffening envelope after cracking was represented by an Izumo's equation, as shown in **Figure 15**.

As for stress - strain relationship under stress reversals, unloading and reloading response of concrete was not linear. The unloading stiffness became lower as the strain at unloading point exceeded the elastic limit. Unloading and reloading curves were represented using equations of high degree while considering those features, as shown in **Figure 15**. The model was derived based on past experimental data.

As for the shear stress - shear strain relationship after cracking of concrete, shear transfer action was expressed by the average shear stress - shear strain relationship along the crack direction. The shear stress - shear strain envelop was determined as a function of the concrete strength, the amount of reinforcement crossing the cracks and tensile strain perpendicular to the crack direction. The model was derived from in-plane shear loading tests of RC panels.

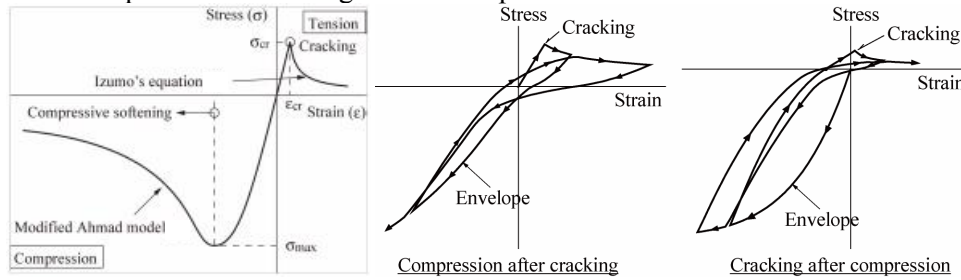


Figure 15. Stress - strain relationship of concrete.

3.2.2 Reinforcement

The stress - strain envelope of reinforcement was assumed to be bilinear. Hysteresis loop was defined by a Ciampi's model.

3.2.3 Ground

For taking into account nonlinear characteristic of the ground, Modified Ramberg–Osgood model was employed on the shear stress – shear strain relationship. Initial shear stiffness G_0 was dependent on the confinement stress, and defined by equation (3.1). The shear stiffness became larger in the proportion to depth from ground surface.

$$G_0 = G_{0m} \times \left(\frac{\sigma_c}{\sigma_{cm}} \right)^{0.325} \quad (3.1)$$

Here σ_c is effective confinement stress to depend on the depth from the ground surface. G_{0m} and σ_{cm} show shear stiffness obtained from the shear wave velocity measured by bender elements, and effective confinement stress at the depth of the measuring points. Hysteresis characteristic under stress reversals was based on Masing rules. Standard shear strain (the strain when the stiffness equal to a half of initial stiffness) was assumed to be 0.1%, and max. damping constant was assumed to be 21.6%.

As for bibliography of the material constitutive model mentioned above, refer to reference [1].

3.3. Analysis results

3.3.1 Results for Case1

Figure 16 compares the time histories of displacement of the footing for the excitation No.d4-d6

obtained from the analysis and the test. **Figure 17** and **Figure 18** show a deformation mode of the whole model, a crack pattern and minimum principal stress contour of the footing at the time of the maximum displacement in the No.d5.

As for the displacement of the footing, it was confirmed that the analysis well reproduced the nonlinear response of the test results, although the displacements of the analysis were slightly little in comparison with that of the tests.

Figure 19 compares the time histories of the displacement of the container for the excitation No.d6. Although the difference between both results appeared slightly, close agreement was obtained for maximum value and waveform between the two.

Time histories of the response acceleration on the superstructure are compared in **Figure 20**. Although periods of the analysis time histories were slightly different from those of the tests, as for the maximum values, good correspondences were obtained between the analysis and the test. As the results, it was confirmed that qualitative tendency of the test results was reproduced by the analysis.

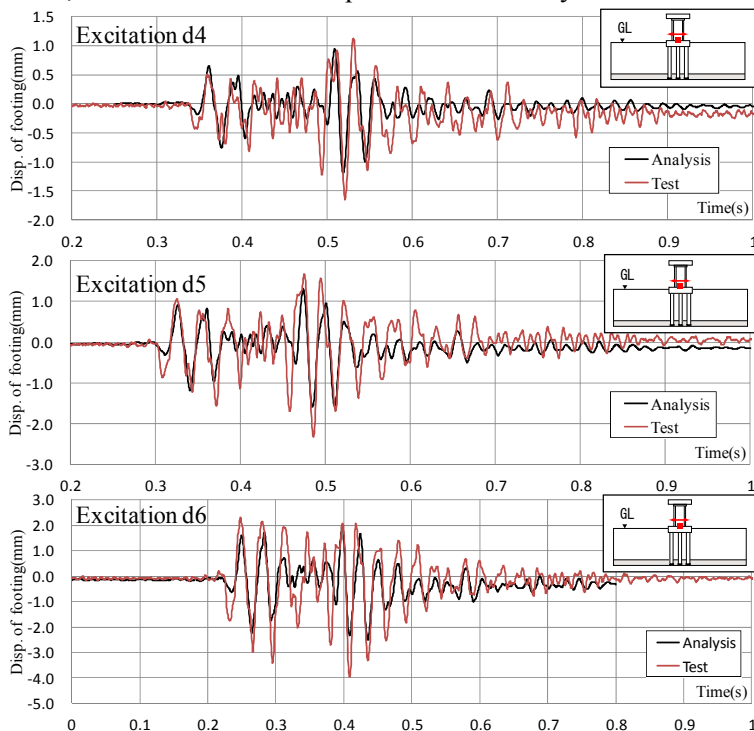


Figure 16. Time histories of horizontal displacement of footing

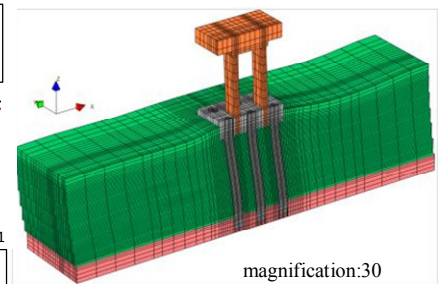


Figure 17. Deformation mode

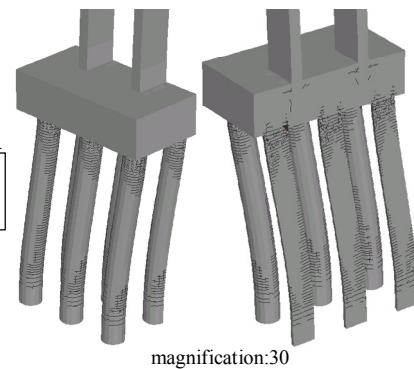


Figure 18. Crack pattern from analysis.

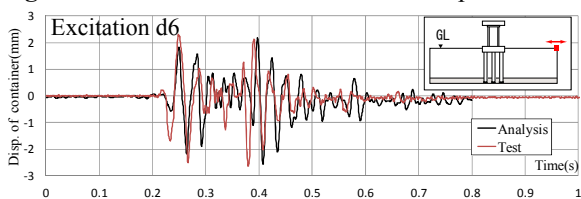


Figure 19. Time histories of displacement of container

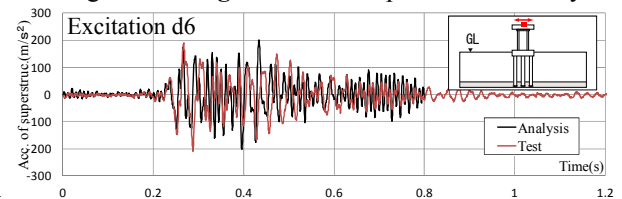


Figure 20. Time histories of acc. of superstructure

3.3.2 Results for Case3

Figure 21 compared time histories of relative displacement of the culvert obtained from the analysis and the test for the excitation No.d6. Time histories of the horizontal displacement at top of the container are compared for the excitation No.d4 and No.d6 in **Figure 22**. Although periods of the analysis time histories were slightly different from those of the tests, as for the maximum values, good correspondences were observed between the analysis and the test. As the results, it was confirmed that nonlinear dynamic response of the test results was reproduced by the analysis as well as the Case1.

Figure 23 shows the rebar yielding condition, minimum principal stress contour, and crack pattern, at the time when the maximum displacement of the culvert occurred. It was found that the rebar yielding and strain concentration appeared at both ends of the pile and both ends of the culvert walls.

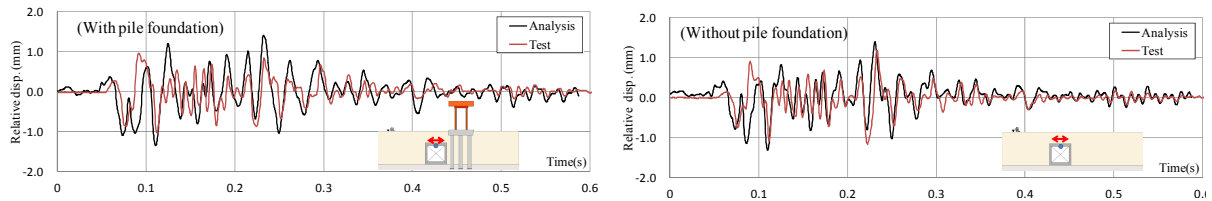


Figure 21. Time histories of relative displacement of culverts (Excitation No.d6)

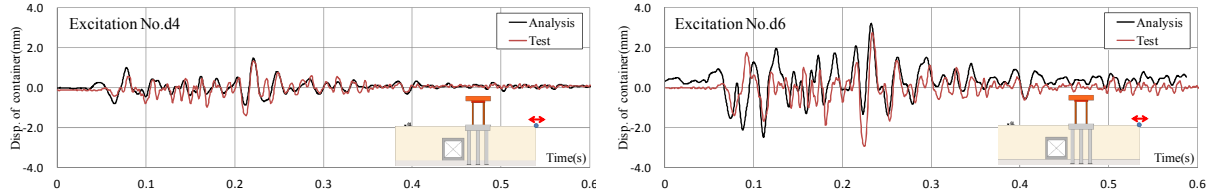


Figure 22. Time histories of horizontal displacement of container

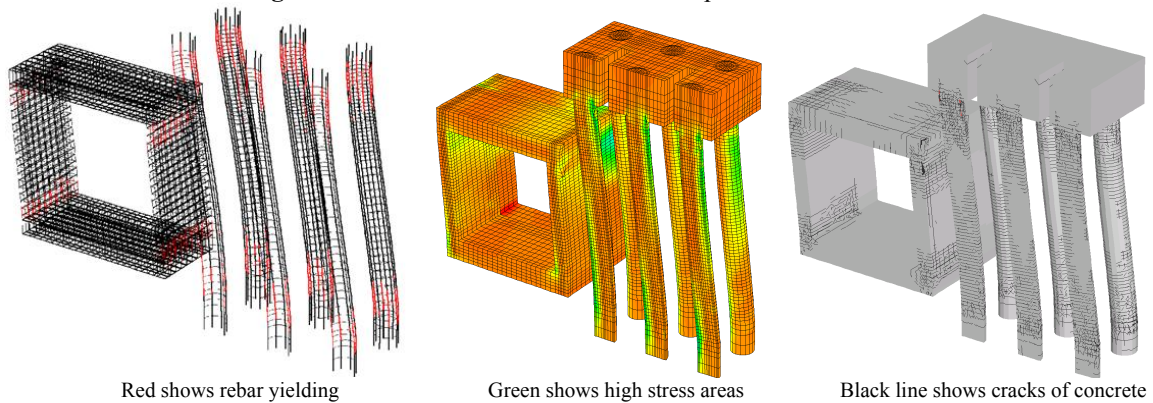


Figure 23. Rebar yield condition, minimum principal stress contour, and crack pattern

4. CONCLUSION

In this study, three cases of centrifuge shaking table test and FEM analyses were conducted here to obtain the fundamental data for nonlinear response of the underground structure and the foundation, and to verify the applicability of the analysis. The conclusions obtained here are as follows.

- 1) By comparing between Case1 with the dry ground and Case2 with the liquefied ground, although the superstructure's acceleration response of Case1 was larger than that of Case2, the footing's displacement of Case2 was remarkably large in comparison with that of Case1. This reason was that the ground stiffness was reduced due to decreasing the effective stress of the ground by raising excess pore water pressure in the Case2.
- 2) By comparing between the two cases with and without a contiguous structure, the influence of a contiguous structure on the response of the box culvert remarkably appeared in the small excitations in which the structure and the ground remained in elastic range. However the influence was not remarkable in the large excitations in which the structure and the ground reached plastic range. The reason was that the difference of stiffness between the structure and the ground became small with yielding of reinforcing bar and cracking of the concrete.
- 3) It was found by the comparison between the test results and the analysis results that the analyses reproduced well the nonlinear response of the structure and the ground for Case1 and Case3 with dry ground. An analysis for Case2 with the liquefied ground will be presented on another opportunity soon.

REFERENCE

- [1] Naganuma, K., Yonezawa, K., Kurimoto, O., and Eto, H. (2004), Simulation of nonlinear dynamic response of reinforced concrete saced model using three-dimensional finite element method. *13th World Conference on Earthquake Engineering*, Vancouver, B.C., Canada, August 1-6, Paper No. 586